Review

Kayn A. Forbes*, David S. Bradshaw and David L. Andrews*

Optical binding of nanoparticles

https://doi.org/10.1515/nanoph-2019-0361
Received September 13, 2019; revised October 18, 2019; accepted October 24, 2019

Abstract: Optical binding is a laser-induced inter-particle force that exists between two or more particles subjected to off-resonant light. It is one of the key tools in optical manipulation of particles. Distinct from the single-particle forces which operate in optical trapping and tweezing, it enables the light-induced self-assembly of non-contact multi-particle arrays and structures. Whilst optical binding at the microscale between microparticles is well-established, it is only within the last few years that the experimental difficulties of observing nanoscale optical binding between nanoparticles have been overcome. This hurdle surmounted, there has been a sudden proliferation in observations of nanoscale optical binding, where the corresponding theoretical understanding and predictions of the underlying nanophotonics have become ever more important. This article covers these new developments, giving an overview of the emergent field of nanoscale optical binding.

Keywords: nano-optics; nanoparticles; nanoscale; off-resonance; optical binding; plasmonics; self-assembly.

1 Introduction

Ever since Kirchhoff's pioneering studies in the mid-19th century, it has been known that the wavelengths of light involved in absorption and emission are determined by the resonance properties of the associated material [1, 2]. Later pursuit by many other notable scientists, including Einstein in 1916, led to an accurate explanation of atomic spectral lines as a phenomenon arising due to resonant absorption and emission [3, 4]. Today, of course, the understanding of the resonance absorption and emission of light by more extended nanoscale systems, such as nanotubes, molecules, quantum dots, etc., is very well understood on the basis of connection with quantum theory.

Soon after the development of the laser in the 1960s, the nonlinear optical effects of an *off-resonant* laser beam also became recognised. For example, a pulsed laser input suffers modification when two or more photons are absorbed [5–7], (as predicted by Göppert-Mayer 30 years before [8]), or transformed into a single lower wavelength output photon [9]. Far less anticipated were the observations of new effects when a moderately intense, off-resonant laser beam is transmitted without loss – i.e. the emergent photons are identical to the incident photons and, therefore, the state of the final light-matter system is identical to the initial one. The earliest example of such an effect is the optical Kerr effect which, in its original concept, involves self-interactions of a single beam [10], wrought by changes in the refractive index. Such changes may be purely electronic, or the result of molecular reorientation in a strong optical field. More generally, the modification of material properties by a throughput beam can lead to effects that are instantaneously evidenced by other, secondary processes. For molecules or particles of nanoscale dimensions, such phenomena – whereby light acts as a stimulus even at an optical frequency where the material is transparent – may be collectively termed "off-resonance nanophotonics".

In current usage, there is no clear distinction between phenomena described as "nanophotonics" and "nano-optics", although the former suggests more prominent significance for quantum and photon aspects. To give a focus to the optical phenomena to be described in the following account it is, therefore, worth recalling some positional forces in optics that are in principle off-resonance in nature. For example, in developments that followed the pioneering work of Ashkin [11] in 1970, optically induced scattering and gradient forces, as well as torques, were observed to act not only on atoms and nanoparticles in optical traps, but also on larger particles in a liquid medium – as in many optical tweezing techniques. Such

***Corresponding authors: Kayn A. Forbes and David L. Andrews,** School of Chemistry, University of East Anglia, Norwich Research Park, Norwich NR4 7TJ, UK, e-mail: k.forbes@uea.ac.uk (K.A. Forbes); david.andrews@physics.org (D.L. Andrews). https://orcid.org/0000-0002-8884-3496 (K.A. Forbes). https://orcid.org/0000-0002-5903-0787 (D.L. Andrews)
David S. Bradshaw: School of Chemistry, University of East Anglia, Norwich Research Park, Norwich NR4 7TJ, UK. https://orcid.org/0000-0002-6458-432X

forces have been found to operate on individual particles through the operation of several distinct mechanisms – see, for example, references [12–19]. In most cases, a classical description of theory may suffice, though the familiar gradient trapping force is clearly a form of off-resonance photon interaction [16, 20].

A phenomenon generally known as "optical binding" has now become one of the most rapidly developing examples of off-resonance nanophotonics [21], although it too can operate by more than one mechanism – determined primarily by the particle size, but also the material characteristics. The term refers to a pairwise force between particles (over and above that of the London dispersion force [22]) due to the presence of an off-resonant laser beam. The mutual interaction *between* particles through optical binding forces can lead to self-organisation into stable, non-contact, dynamic configurations of matter. Thirunamachandran [23] originally predicted the existence of this laser-induced inter-particle force in terms of molecule-photon interactions in 1980. The concept attracted much further theoretical [24–28] and experimental [21, 29–32] interest in the following years, at first mainly in relation to microparticles. While the initial works involved study of the attraction between two particles (or repulsion, despite the term "optical binding"), it was later found that multiple particles can be held together by the off-resonant light in an "optical matter" configuration [30].

Although the vast majority of studies in the field are concerned with microscale optical binding, an extensive amount of research in the last 10–15 years has been centred on optical binding between nanoparticles. This nanoscale optical binding is the focus of the following Review, where we provide an overview of both experimental and theoretical studies extending to the latest, novel effects that arise on input of structured light, irradiation of chiral nanoparticles, and the role of plasmonics to name just some of the key developments.

2 Optical binding

2.1 General description

The laser-induced optical force that exists between two or more micron- or submicron-sized particles, when subjected to a moderately intense off-resonant laser light at optical frequencies, is commonly known as optical binding. For studies in pursuit of optical nanomanipulation, it is worth recognising a need for those particles to also be individually supported by a localising force, most often the force of optical tweezers or trapping by the self-same laser beam. For example, in the case of laser tweezers the particles are localised in a microscale volume, commonly supported in a passive liquid support medium to offset the effect of gravity [33]. It is with such particles, already held almost stationary in an optical field, that optical binding exerts its effect as a stabilising influence on inter-particle separations. This is an effect that can still be significant at inter-particle separations on the order of a few multiples of the optical wavelength. For particles of a dimension significantly smaller than the wavelength, it is important to recognise that the capacity to individually steer, by conventional optical tweezer forces, is to some extent compromised by such pair (or larger ensemble) forces, also induced by the presence of the trapping beam. More significant, however, is the capacity for multiple particles to be held together by light – in stable and non-contact arrays of varying geometries. The exploration of this facet has led to optical binding becoming an immense field in its own right [21, 32, 34], as well as an indispensable tool in the area of optical manipulation [20].

The initial predictions of the effect in seminal theory by Thirunamachandran [23] was followed by the pioneering efforts of Burns et al. [29, 30], who first coined the term "optical binding", and experimentally demonstrated the effects of light-induced forces between micro-sized spheres of polystyrene, triggering a proliferation of activity in the field. They employed the semiclassical explanation of optical binding, whereby the throughput light is considered to cause fluctuating dipoles in each particle, inducing their mutual interaction. The fluctuations are generally out-of-phase due to their different positions in the beam, generating an essentially sinusoidal dependence for the dipole-dipole interaction energy, as a function of displacement. This coupling is, of course, modified by an inverse power dependence due to the fall-off of the dipole radiation field with distance. Despite its simple appeal, this classical picture fails to include the retardation features that naturally emerge from the quantum description. It is indeed an important feature of optical binding that its angular and distance dependence vary in different regions of displacement. In the quantum electrodynamical (QED) viewpoint, which is more suitable and rigorous for the nanoscale, the mechanism consists of four distinct, correlated photon events: annihilation of an input photon at nanoparticle A, virtual photon mediation of the interaction between A (creation site) and a second nanoparticle B (annihilation), and stimulated re-emission of an input-mode photon at B. The input and output photons are identical.

This scheme is illustrated in Figure 1. Note that the theory provides for the virtual photon to propagate with quantum uncertainty in its wave vector, consistent with the short lifetime and small distance of propagation [35].

Since the energy and direction of the input photon equals that of the output photon, the radiation and optical material suffers no change of state in the overall mechanism. The binding force, therefore, can be seen as the modification of the Casimir-Polder (dispersion) forces between nanoparticles in the presence of the off-resonant, passive radiation. These binding forces can significantly increase inter-particle forces, without altering the modal composition of the incident field: the off-resonant beam may be thought of as an optical catalyst [36–40].

For two nanoparticles A and B, with scalar frequency-dependent (dynamic) molecular polarisabilities $\alpha(\omega)$, and an inter-particle displacement vector $\boldsymbol{R}$, the optical binding potential energy in the electric-dipole approximation [41] takes the form in summed index notation (for light with wave vector $\boldsymbol{k}$):

$$\Delta E = \left(\frac{I}{\varepsilon_0 c}\right)\alpha_{\mathrm{A}}(\omega)\alpha_{\mathrm{B}}(\omega)\bar{e}_i^{(\eta)}e_j^{(\eta)}\,\mathrm{Re}V_{ij}(k,\boldsymbol{R})\cos(\boldsymbol{k}\cdot\boldsymbol{R}) \qquad (1)$$

where I is the input beam intensity, $\boldsymbol{e}$ are polarisation vectors for the mode $(\boldsymbol{k}, \eta)$ – with the overbar denoting complex conjugate – and the retarded dipole-dipole virtual photon propagation tensor takes the following, complete form [42], applicable to arbitrary separations R:

$$V_{ij}(k,\boldsymbol{R}) = \frac{\mathrm{e}^{ikR}}{4\pi\varepsilon_0 R^3}[(\delta_{ij}-3\hat{R}_i\hat{R}_j)(1-ikR)-(\delta_{ij}-\hat{R}_i\hat{R}_j)k^2R^2] \qquad (2)$$

Here, either the first (R^{-3}) or the final (R^{-1}) term will dominate as the asymptotic form under important limiting conditions – the near- and far-fields, respectively. In the latter, where the inter-particle coupling is mediated by a fully retarded radiation field, the R^{-1} distance-dependent decay may be considered a novelty when compared to the much more rapidly decaying Coulomb (R^{-3}) and dispersion (R^{-7}) interactions.

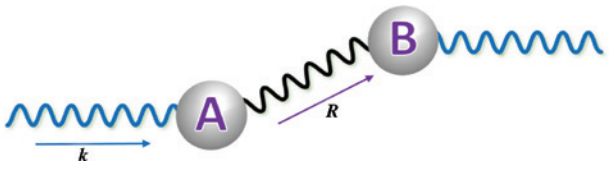

Figure 1: Optical binding between nanoparticles A and B separated by a displacement vector $\boldsymbol{R}$.
Identical input and output photons of wave vector $\boldsymbol{k}$ are depicted in blue, a virtual photon in black.

Before proceeding further, it is useful to highlight a few more general properties of Eq. (1). First, the binding energy is linearly dependent on the incident laser intensity; it is also dependent on a product of the polarisabilities of both A and B. (Notwithstanding their associated dispersion properties, the magnitude of each polarisability may be considered broadly proportional to the physical volume of the corresponding particle, or the volume over which outer electronic orbitals extend.) Furthermore, the binding energy is dependent on the direction of incident light propagation and the electric field polarisation relative to the separation of the particle pair. In passing we note that A and B need not necessarily be identical; asymmetric interactions between unlike particles introduce further novelties [43–45]. Moreover, when either one or both of the nanoparticles is polar, there is an additional static contribution [22, 46] to Eq. (1) – but it has a monotonic, non-oscillatory form and, therefore, cannot itself engender positions of configurational stability.

It is to be stressed that from the simple results of Eqs. (1) and (2), applicable to optical fields with arbitrary polarisation and beam geometry, a plethora of further analytical theories can be derived for numerous scenarios, such as optical binding in gaseous and liquid systems, and/or longitudinal $\boldsymbol{k}\,||\,\boldsymbol{R}\equiv\boldsymbol{e}^{(\eta)}\perp\boldsymbol{R}$ or transverse (lateral) $\boldsymbol{k}\perp\boldsymbol{R}\equiv\boldsymbol{e}^{(\eta)}\,||\,\boldsymbol{R}$ binding. The forces experienced by particles under such conditions are given by the negative derivative, with respect to R, of the potential energy results: for simplicity of dealing with scalar quantities, we shall focus on potential energy expressions. In general, the strongest binding forces and most stable configurations arise when the incident laser is polarised perpendicular to $\boldsymbol{R}$, a condition that is always satisfied when the particles lie along or parallel with the beam axis (see Figure 2). For the vast majority of stable optical binding configurations, the magnitude of the inter-particle displacement is characteristically similar to the incident wavelength $\boldsymbol{R}\approx\lambda$; for more stable binding interactions that can occur with larger micron-sized particles, equilibrium values of $\boldsymbol{R}$ can take on multiple values.

While Eqs. (1) and (2) are exact if A and B are freely isolated particles, a more experimentally realistic scenario accommodating the dielectric effect of a surrounding medium (e.g. colloidal suspensions) can be accounted for with a trivial extension of the QED theory [47–49], accounting for the refractive index of the support medium. The most significant aspect is simply that the wave vector $\boldsymbol{k}$ is multiplied by the refractive index of the support medium for the laser wavelength, serving in effect

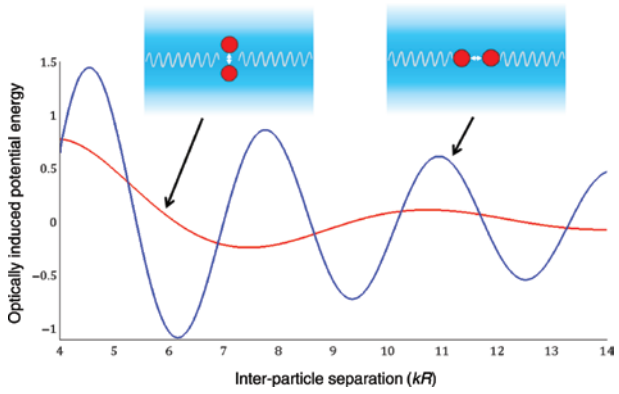

Figure 2: Graph of optically induced potential energy (with arbitrary scale) against inter-particle separation measured in terms of kR, for longitudinal (blue line, as depicted in inset diagram) and transverse (red line, also shown) optical binding; k is given a typical value of 3×10^{-7} m^{-1}.
Notice that both oscillating curves are damped as the separation distance increases.

to reduce the length of the stable inter-particle distances by the same factor [50].

In general, studies on optical binding are concerned with either nanoparticles (such as nanospheres, nanotubes and small molecules) or microparticles (comparable to or larger than the wavelength of incident light) and, until the present, the number of experiments on the latter has substantially outweighed those on nanoparticles. This is primarily due to the fact that the optical binding force scales proportionally with particle volume (or, alternatively, through particle radius a as a^6) and it is, in consequence, more easily observed with larger particles that also have much slower Brownian motion – the latter representing a phenomenon that is disruptive to both optical trapping and optical binding. Experiments by Demergis and Florin [51] in 2012 proved the advantage of the large polarisabilities (due to localised surface plasmon resonance) in Au nanoparticles, such that the optical binding between particles with diameters of 200 nm can become "ultrastrong". In the following year, Yan and co-workers [52] optically bound Ag nanoparticles together as small as 40 nm in diameter – thus, bringing experimental studies on optical binding into the Rayleigh regime. Theoretical studies concerned with nanoparticles are clearly becoming increasingly more important as optical binding experiments enter the Rayleigh regime, alongside a rapid growth in advances in nanophotonics [53].

Following the above presentation of recent work on optical binding forces and the general results that can be applied to them, we now progress to survey the recent studies that invoke suitable modifications to Eq. (1) – in order to elucidate the rich landscape of optomechanical opportunities afforded by optical binding at the nanoscale.

2.2 Observing nanoscale optical binding

As mentioned above, optical binding with nanoparticles is notoriously sensitive to thermal fluctuations and Brownian motion, the effect of which rapidly increases with every decrease in particle size. Indeed, the resultant lack of stability for small particle pairs and assemblies has dictated that the overwhelming majority of experimental studies have, until recently, involved particles of micron size. However, the stability of optical binding arrays can be improved by exploiting extrinsic factors, i.e. the characteristics of the incident laser such as intensity and spatial profile [54], and by intrinsic factors related to the configuration and material composition of the particles. Before proceeding further, we therefore outline some of the strategies that can be used.

Nan and Yan [55] have experimentally investigated the spatial and temporal stability of gold nanoparticles using polarisation modulation, verifying many well-established results concerning the spatial stability of optical binding, such as the fact that light polarised transverse to the inter-particle displacement vector $\boldsymbol{k}\,||\,\boldsymbol{R}\equiv\boldsymbol{e}^{(\eta)}\perp\boldsymbol{R}$ affords a much higher probability of the nanoparticles occupying a more stable potential well. This was recognised in the original work by Thirunamachandran [23] (and it is indeed a paradigm in optical binding studies, having been observed in many experiments). Similarly, the observation that the addition of particles to a chain increases the depth of potential wells, for particles already in the chain – i.e. particles closer to the centre are more stable than those further away – has been frequently observed. One key innovation is a modulation between parallel and perpendicular polarisations, each pushing particle pairs towards a different relative position. The frequency of modulation allows inter-particle separation to be fine-tuned; the higher the modulation frequency, the more dominant is the configuration due to transverse polarisation.

The first experimental observation in the nano-regime, by Demergis and Florin [51] as mentioned previously, was made possible because of the localised surface plasmon resonance properties of metal nanoparticles and enhanced trapping stability brought about by their standing wave optical line trap (SWOLT) [56] – which relies on interference of the incident light with its reflection to obviate destructive axial scattering forces. A further novelty of their study was an observation of the ability for smaller particles, which would normally spatially fluctuate, to effectively become anchored in the presence of larger particles (Figure 3). This is an effect that is again consistent with theoretical determinations using QED [57].

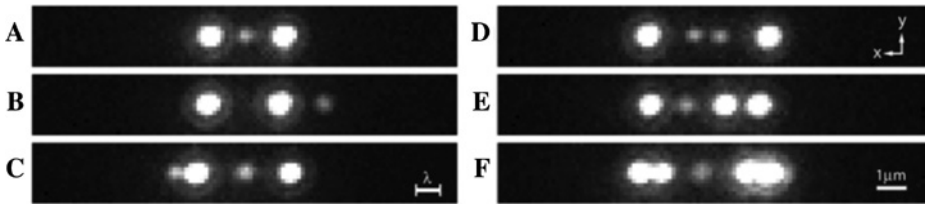

Figure 3: Assisted trapping of nanoparticles using optical binding forces.
Two gold nanoparticle sizes (200 nm and 10 nm) trapped in water and aligned in a standing wave optical line trap (SWOLT), using a 1064 nm wavelength laser at approximately 200 nm above a reflecting coverslip surface. Individually, smaller particles exhibit large fluctuations along the *x*-axis; using the larger particles as anchors, the small particles become confined due to the strong optical binding forces. Scale bar $\lambda = 800$ nm. Reproduced with permission from [51].

Interferometric traps such as the SWOLT rely on the interference between optical fields where, compensating for radiation pressure, certain locations experience enhanced optical intensities and gradients, leading to stronger electrodynamic interactions. One of the first methods to utilise such methods in optical binding constructed them from a single beam and its reflection from a gold nanoplate mirror [54]. The enhanced binding (and trapping) forces were not attributable to plasmonic enhancement, but rather a restricted thermal motion, with reduced inter-particle fluctuations and a four-fold enhancement of the intensity, due to the interference.

One issue with standing wave interferometric traps is that nanoparticles hardly enter the trapping fields because of a lack of radiation pressure; working with large assemblies of optical matter, therefore, remains a challenge. Nan and Yan [58] have highlighted how to overcome the issue of compensated radiation pressure by using a silver nanowire interferometric optical tweezer approach, where both the optical trapping and binding forces of metallic and dielectric nanoparticles can be significantly enhanced *in situ*. On laser illumination, the silver nanowire acts as a plasmonic antenna, producing a three-dimensional (3D) interferometric optical field that is able to strongly influence the electrodynamic interactions among nanoparticles perpendicular to the nanowire. This method affords the achievement of polarisation-controlled, large-scale, and stable optical matter arrays comprising up to 60 nanoparticles – the largest nanoparticle-based optical matter assembly reported to date (Figure 4).

A follow-up study by the same authors showed that, by using a dual-beam system, free-standing strongly trapped metal nanoparticle chains with tuneable lengths are, in fact, better at 2D optical assembly than nanowires, as both the trapped chain and loosely bound nanoparticles sit in the same plane, optimising the interferometric fields [59]. This lateral interferometric optical field is distinctly different to those discussed previously, and it affords

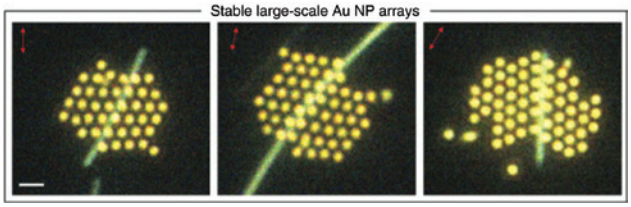

Figure 4: Dark-field images of silver nanowire-assisted optical assembly of multiple silver nanoparticles into stable hexagonal lattices.
The angle of polarisation is 30° to the vertical plane of the image. Scale bar is 1 μm. Reproduced with permission from [58].

significant control over the optical matter – in particular, a strong dependence on the trapped particle chain length dictates the strengths and configurations of the optically bound particles.

Jaquay et al. [60] first showed that gold nanoparticles in a light-assisted, templated self-assembly 2D trap form 1D periodic patterns, arising from the competing trapping and optical binding forces. From an optical binding perspective, it is important to note that a previous study on polystyrene particles showed that inter-particle interactions play almost no role in the patterns observed [61]: this stems, of course, from the large polarisabilities and binding interactions between metal nanoparticles. In recent work, the same group has highlighted how 2D square lattice traps induce 1D nanoparticle chains, whereas 2D *hexagonal* lattices allow periodic 2D particle arrays to be formed with over 50 gold nanoparticles [62].

2.3 Potential energy landscapes and multi-particle assembly

Optically induced inter-particle (or optical binding) potentials can be revealed in pictorial 3D scalar fields, commonly termed potential energy landscapes [50, 63, 64].

One such landscape, in which a spherical nanoparticle is positioned at the origin, is exhibited in Figure 5. In these landscapes, the potential wells of local energy minima correspond to stable optical binding, while the maxima reveal energetically unstable configurations.

Both attractive and repulsive optical binding forces operate to impel particles across the potential landscape to stable separations of local energy minima. As predicted in a theoretical analysis in 2010 [65], the occurrence of multiple local minima in such potential energy landscapes indicates the possibility of configuring a variety of geometrically distinct particle assemblies, such as chains, triangles, rings, and hexagonal arrays, and the probability of any particular formation is partially dependent on the initial conditions. One immediately evident configuration that consists of particle chains along a particular axis (the *y*-axis of Figure 5), corresponding to longitudinal optical binding [66], is an important structural motif in optical binding studies. Another recent theoretical study has shown – among other details – that by introducing surface plasmon polariton interference, the separation between bound nanoparticles (and, thus, the energy minima in the potential landscape) can be significantly reduced, even surpassing the diffraction limit to which optical binding is typically subject [67].

In multi-particle assemblies, interactions between all the particles create a rich and complicated potential energy landscape. Although non-pairwise couplings exist, the optical forces are dominated by pair interactions (rather than three-body interactions, etc.) and a simple sum of these interactions often suffices to explain the formations of optically bound multi-particle arrays. The most expedient way of studying the energetics associated with the arrangements of three or more particles is by positioning them in the minima of a suitable template, such as Figure 6.

As can be seen in Figure 6, the number of viable minima has increased for the multi-particle systems, engendering an increase in the number of potentially stable arrays and configurations. However, this increased number of arrays may lead to disorder in assemblies of larger numbers, as many local energy minima are available, and the potential wells are often not deep enough to maintain stability against thermal fluctuations. Nan et al. [68] have highlighted a method of obtaining a disordered-to-ordered array transition for metal and dielectric nanoparticles, whereby the optical binding strength is a crucial component, but still exhibits frequent transitions between differing structures. The fluctuating dynamics that operate within such assemblies has been dramatically illustrated in work by Kudo et al. [69] on large assemblies of swarms of around 1000 gold nanoparticles.

Computational and theoretical simulations play a large role in optical binding studies, where they are used to compare and quantify experimental results or provide predictive insight. In particular, the finite-difference time-domain numerical method is regularly used to solve Maxwell's equations and simulate the electrodynamics [70]. The availability of off-the-peg commercial software for such applications nonetheless tends to mask its reliance on classical formulations of the electrodynamics, potentially obscuring quantum effects and intrinsic

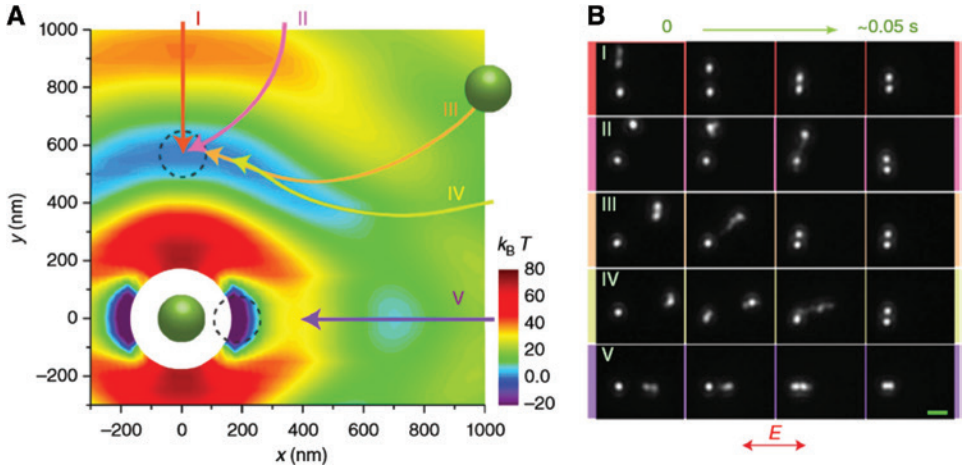

Figure 5: Path-dependent self-organisation of two 150 nm diameter Ag nanoparticles, using 800 nm radiation.
(A) Electrodynamic potential energy surface and illustrated paths of the second particle entering the optical fi El. Units of $k_B T$ assume $T = 293$ K. (B) Corresponding optical images from five experiments in which the second particle enters from different directions. Scale bar, 1 µm. Reproduced with permission from [64].

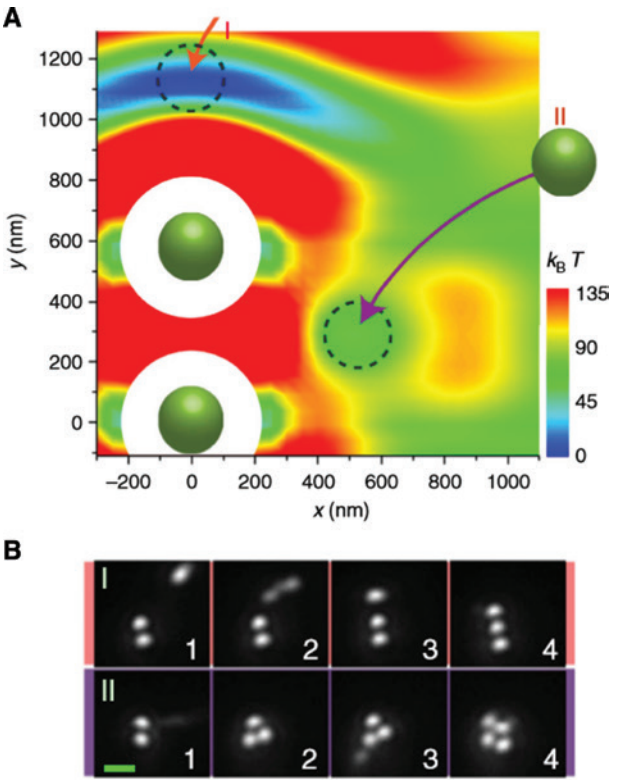

Figure 6: Path-dependent self-organisation of three 200 nm diameter Ag nanoparticles.
(A) Potential energy surface of a third Ag particle joining an optically bound dimer in an optical field with 800 nm wavelength, and pathways of the third particle. (B) Corresponding images of two experimental events in which the third particle enters the optical field from different directions. Images II-3 and II-4 show the addition of a fourth nanoparticle. The relative time points of the images in I are 0 s, 0.01 s, 0.02 s, and 1.82 s while those in II are 0 s, 0.01 s, 0.66 s and 0.67 s, respectively. Scale bar, 1 μm. Reproduced with permission from [64].

uncertainties. This shortcoming is less significant in computational work where particle motions are addressed. One example is the important Langevin dynamics that relate to motions of the nanoparticles in solution. As such, an electrodynamics-Langevin dynamics (ED-LD) approach has been developed to deal with the complicated mechanics of optical binding [71]. One particular insight afforded by the ED-LD approach has been to highlight the role of the shape and dimensions of the incident beam, with tight focusing proving to exert an effect on the equilibrium binding separations between particles. This work has also highlighted the important role that surface charges play in optical metal nanoparticle self-organisation.

Another insightful study on self-assembly achieved a high fidelity correlation between computational simulation and experimental evidence of multi-nanoparticle configurations [72], as illustrated in Figure 7. A further exploitation of the ability to create multi-particle assemblies with optical binding forces is the creation of a self-healing optical membrane, consisting of 150 non-contact particles, producing a reflective surface that can be used as a laser-trapped mirror [73].

2.4 Structured light

The incident laser beam is itself an element that may be spatially tailored to add an additional element of control in the manipulation of nanoparticles. It is worth pointing out that the term "structured light" in such a connection here specifically refers to the properties of an incident beam (in some other work the terms "structured or shaped light fields" are used to denote the interference of incident and scattered light). Beyond simple focusing, the application of a beam with intensity- and phase-structure offers a further experimental degree of freedom. Indeed, structured light in the form of a zero-order Bessel beam was used in the first experiment to exhibit optical binding in the Rayleigh regime [52]. An especially important class of structured light beams are orbital angular momentum (OAM)-carrying optical vortices [74–76]. These "twisted" beams have seen widespread utilisation in a plethora of areas including free-space information transfer, microscopy, and imaging, although, to-date, the vast majority of studies have exploited their unique properties in opto-mechanical forces and manipulation [77–83].

Due to the ability of a sufficiently intense laser beam to trap nanoparticles within its cross-section, a study of the optical binding forces between nanoparticles trapped within an optical vortex is of added interest. The most widely utilised class of twisted laser beams are Laguerre-Gaussian (LG) modes, the Gaussian beam profile of which is tempered by an associated Laguerre polynomial of index p (indicating an integer number $p+1$ of intensity rings, or radial nodes), and order ℓ, which is also known as the topological charge (a measure of the amount of beam "twist"): the value of ℓ also signifies an OAM of $\pm\ell\hbar$ per photon. For an LG mode with a single ring ($p=0$), the possible arrangements of optically bound multi-particle arrays is determined by optical forces that are sensitive to both ℓ and the azimuthal displacement angle between the nanoparticles [84]. For such beams, it emerges that there are ℓ energy minima and $\ell-1$ maxima on the cylindrically symmetric potential energy surface. The complexity rises further when an increasing number of nanoparticles are bound within the beam. For odd values of $\ell>1$, only a local minimum (though not the energetically most favourable one) arises for nanoparticles at diametrically opposed

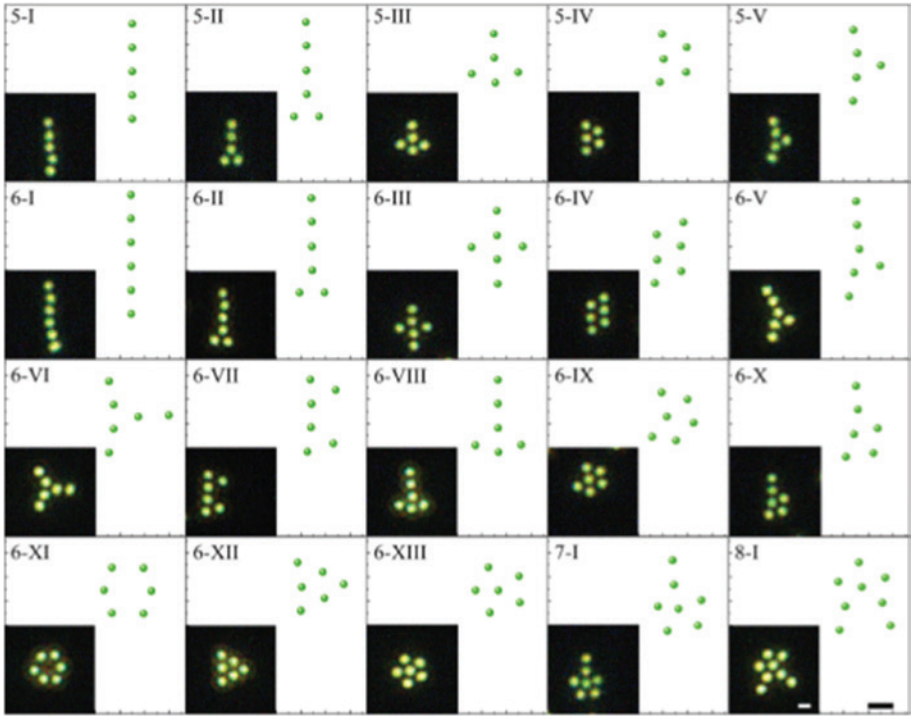

Figure 7: Predicted and observed optical matter isomers consisting of up to eight Ag nanoparticles.
The plotted schematics are the equilibrium configurations predicted by simulations, while the optical images show the corresponding clusters observed in the experiments. The two scale bars in the last panel are 600 nm. Reproduced with permission from [72].

positions within the beam cross-section – which has been observed experimentally [85]. For even values of ℓ, a local *maximum* occurs for nanoparticles opposite one another. However, for any value of ℓ, the depths of local minima close to the equidistant positions are greatly outweighed by the absolute minimum (and those of similar depth nearby) that corresponds to clustering of the trapped nanoparticles, as depicted in Figure 8. It should be made clear here that this nanoparticle clustering within the cross-section of the LG beam is completely distinct from the optical spanner (wrench) effect that involves particles travelling around the ring, due to OAM transfer to them [79].

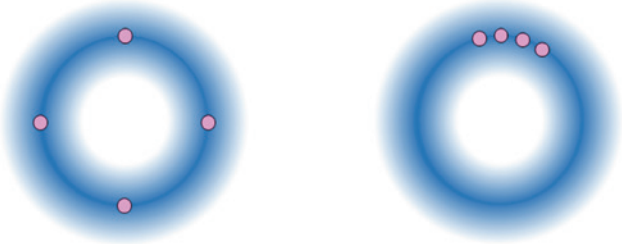

Figure 8: Diagrams showing nanoparticles trapped in the cross-section of a Laguerre-Gaussian beam.
While, on symmetry grounds, it might be expected that the nanoparticles will settle at positions equidistant from each other (left-hand diagram), optical binding produces a clustering effect (right-hand diagram).

Experimental studies of optically bound silicon nanowires in circularly polarised LG beams have exhibited a rich interplay between the OAM and spin angular momentum, allowing the bound nanowires to orbit around the beam as well as spin on their own axis [86]. The dynamics of metal nanoparticles, optically bound in an OAM-possessing optical ring vortex, have also now been studied experimentally [87, 88]. Figliozzi et al. [87, 88] created a special optical ring vortex, the intensity profile and radius of which are independent of ℓ, by utilising a gold nanoplate mirror to produce interferometric fields in a retroreflection geometry, creating a series of optical ring traps along the optical axis. They trapped silver nanoparticles within the rings, and studied the variation of the optical binding forces as a function of their ring location. Firstly, they observed that particles become preferentially optical bound at separations that correlate to a polarisation transverse to their displacement vector (a characteristic property of optical binding systems, as previously noted); furthermore, the inter-particle separations were themselves found to be approximately integer values of the incident wavelength. Studying the influence of the gold nanoplate by replacing it with a glass cover, they also

discovered that the gold nanoplate significantly increases the optical binding forces due to a fourfold increase in intensity (see Figure 9). Importantly, Figure 9 also highlights that when the optical force is increased through larger values of ℓ and hence larger OAM, this increases particle fluctuations which compete with the attractive binding forces – and the consequential broadening of the distributions leads to only the first site (0.6 μm) being populated at large ℓ. The dynamics of inter-particle separations were also simulated, and it was found that for increasing ℓ, the probability density for other, less stable binding configurations emerges, fully agreeing with the experimental results of Figure 9: by increasing the topological charge and OAM, optically bound particles separate more easily from their initial, most stable separation.

Another important manifestation that stems from structured light is the role of phase gradients [89–91]. Such gradients are well known to be important in trapping single particles, but it has recently been highlighted how the pairwise binding interactions between silver nanoparticles are dependent on the magnitude of the incident phase gradient, specifically the location, strength, and number of stable binding locations. For small phase gradients, the binding between the pairs is modulated by a dependence on inter-particle separation; for large gradients, the symmetry of the interaction is broken, and this significantly alters the potential energy landscape. Clearly, in summary, the growing use of structured light beams offers a new dimension for the optical control of multi-particle assemblies bound by light.

2.5 Non-spherical nanoparticles

In most experimental and theoretical studies of optical binding, the nanoparticles are spherical. However, because binding forces depend on the polarisability of the particles – a physical property that is a highly sensitive to the direction of the applied electromagnetic field – non-spherical and anisotropic nanoparticles can have enhanced attraction along certain dimensions, and theory shows that this can lead to substantially different interaction dynamics [92].

The first experimental study of optical binding with anisotropic, non-spherical nanoparticles occurred as recently as 2018, where arrays of optically bound gold disc-like nanoplates were formed and found to exhibit very different interactions and dynamics than nanospheres [90]. In particular, the major differences between the nanoplates and the nanospheres were that the former exhibit smaller separations R between one another, and that they also possess much slower transport and correlated drift motions than nanospheres. These differences stem from the large size and anisotropic nature of the nanoplatelet, causing higher-order magnetic quadrupole and electric octupole interactions and interferences with the field becoming more important than they are in small spheres – where electric dipole interactions vastly outweigh any other contributions, in general. Furthermore, the multipolar plasmon modes of the nanoplates induce both near-field (see Section 2.8) and characteristic longer-range optical binding interactions.

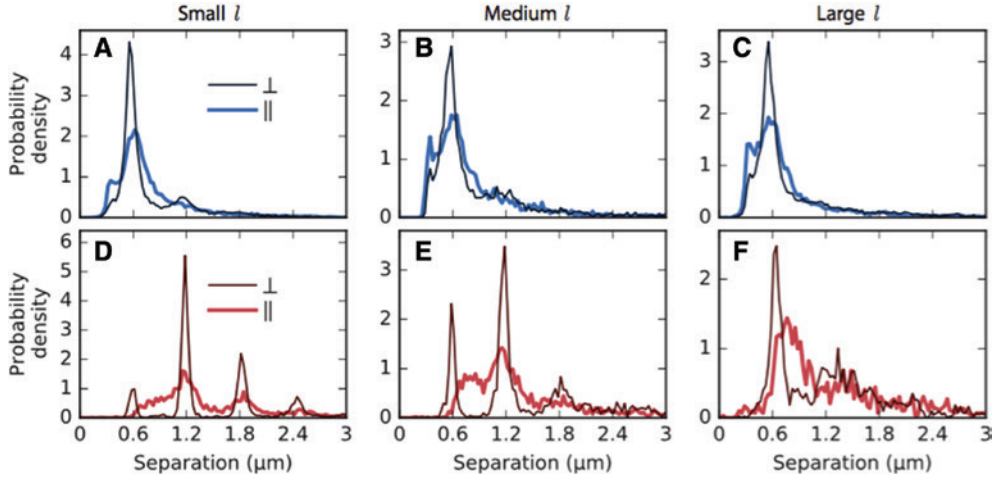

Figure 9: Conditional probability distributions of nearest neighbour nanoparticle separations grouped into categories of applied forces. (A), (D) small ($\ell = 0 - 2$), (B), (E) medium ($\ell = 3$), and (C), (F) large ($\ell = 4 - 5$) for experiments with particles over glass (blue, top row) and over a silver nanoplate (red, bottom row). Each panel shows distributions for particle pairs parallel (thick light-coloured curve) or perpendicular (thin dark-coloured curve) to the polarisation. Reproduced with permission from [87].

One particularly important class of nanoparticles are those with cylindrical symmetry, such as carbon nanotubes. The latter are unique nanostructures that offer a remarkable combination of conductive, steric and material characteristics [93, 94], which can be readily trapped and manipulated by optical tweezers [15]. These, therefore, represent an interesting optical binding system to study, although the theory is complicated by an expansion from three to seven degrees of geometric freedom. From fundamental theory, detailed laser-induced forces have been determined for single-walled carbon nanotubes [95]. In this work, two distinct schemes were selected: a pair of parallel nanotubes irradiated in a fixed direction, and a pair with arbitrary mutual orientation that are free to tumble in the input field. Due to variations in geometry, the optical binding forces prove to be either attractive or repulsive, and for nanotubes of length 200 nm and radius 0.4 nm, separated by 2 nm in the presence of the off-resonant beam of 10^6 W m^{-2}, values of the induced force range from 10^{-6} to 10^{-9} N. The unique electronic properties of carbon nanotubes mean that, for similar separation distances, the calculated optical binding forces between the pair can greatly exceed the known value of the corresponding Van der Waals interactions [96].

Further studies on cylindrical objects include a detailed and rigorous computational study on dielectric nanowires. In their work, Simpson et al. [97] discovered that optical binding forces allow for the formation of ladders of nanorods, alongside the ability to rotate and translate them, providing the ability to perform the necessary manipulations of nanoparticles in intricate tasks required by optically driven micromachines. A recent study has experimentally shown that the optical binding forces between silicon nanowires trapped in counter-propagating beams play a role in rotational binding effects [86].

Another pair interaction that can be modified by the optical binding potential occurs in molecular solids, and is manifest through microscopic mechanical effects. A particularly appropriate structure consists of an arrangement of parallel, cylindrical molecules, as found in solids comprised of poled polymers or smectic/nematic liquid crystals. Irradiating the solid with linearly polarised light results in a contraction parallel to the polarisation of the laser beam and an expansion in the other two dimensions, both linearly dependent on the irradiance of the laser. This optical electrostriction – compression and expansion due to optical binding forces – leads to a deformed solid with an increased volume, signifying a change in local density, and thus a change in the local refractive index that scales linearly with the irradiance of the incident beam: as such, it represents an optomechanically induced intensity-dependent refractive index. This optical electrostriction [98] due to interactions between the radiation field and matter differs from the electrostrictive effect connected to static electric fields, and contributes to a phenomenon dominated by the much more widely known optical Kerr effect [99].

As observed earlier, the polarisability of a molecule roughly scales with its volume, and the quadratic dependence of the optical binding forces on the polarisability dictates that observing and quantifying the laser-induced intermolecular force for small dielectric molecules can be technically demanding. Van der Waals dimers are weakly bound pairs of molecular structures with large moments of inertia due to the long intermolecular bond holding the pair of molecules together. Due to this large moment of inertia, these dimers are readily identifiable by high resolution microwave spectroscopy, one of the most widely studied species being $(HCN)_2$. In the presence of the off-resonant radiation, the intermolecular bond potential has been shown to be modified by the laser-induced optical binding force, the sum of the two producing an effective potential [98]. The reported rotational constant for $(HCN)_2$ is 0.0584 cm^{-1} [100] – the change in equilibrium bond length induced by a modest laser irradiance of 10^{12} W cm^{-2} will cause the dimer bond length to extend by 1.72 pm, which produces a new rotational constant of 0.0579 cm^{-1} – a difference of about 1%. This is experimentally very significant, and well above the bounds of error in microwave spectroscopy, and offers one way to quantify the optical binding effect in small molecules.

2.6 Chiral effects

The origin of the optically induced binding energies discussed so far have primarily involved only the dominant electric-dipole (E1) form of interaction with the radiation field. However, once we entertain anisotropic and low-symmetry particles, such as most molecules, other multipolar interactions with the field must be considered. The dominant E1^{2}E1^2, or alternatively "α^2" couplings such as Eq. (1), are insensitive to any chirality (or handedness) of the interacting molecules, but chiral species allow for the interferences of higher-order transitions. In particular, the incorporation of magnetic dipole (M1) interactions produces chiroptical (or discriminatory) effects.

It was Salam [101] who first highlighted how allowing for a single M1 interaction at each of a pair of chiral molecules A and B, produces a chiroptical effect dependent upon the product of the mixed electric-magnetic

dipole polarisability tensor: we term this "*GG*" coupling. The $\boldsymbol{G}$ tensor – an E1M1 analogue of the polarisability – is well known in the study of chiroptical phenomena, as it is responsible for processes such Rayleigh and Raman optical activity, discriminatory dispersion [102, 103] and optical trapping forces [104, 105]. For any one chiral species of a pair of enantiomers A and B, $\boldsymbol{G}$ has a value that is the opposite sign of that for the corresponding optical isomer: $\boldsymbol{G}(\mathrm{A}) = -\boldsymbol{G}(\mathrm{B})$. The binding energy for a pair of right-handed enantiomers differs from that between the right-handed and left-handed forms, for example: in general $\mathrm{RR} = \mathrm{LL} \neq \mathrm{RL} = \mathrm{LR}$. The result is also identical for incident light that is either linearly-polarised or circularly-polarised, i.e. $\Delta E^{(GG)}_{\mathrm{Lin}} = \Delta E^{(GG)}_{\mathrm{Circ(L/R)}}$. This chiroptical contribution to the binding force is typically weaker than the dominant α^2, typically by a factor of around 10^{-6}.

More recently, a mechanism that involves M1 coupling at only one of the chiral molecules has been reported [106] – this corresponds to a much larger discriminatory optical binding force, enhanced by an order of 10^3. By utilising the fact that chiral molecules can possess both a $\boldsymbol{G}$ and $\boldsymbol{\alpha}$ polarisability, a discriminatory optical binding energy that couples the $\boldsymbol{G}$ of one enantiomer with the $\boldsymbol{\alpha}$ of the other is possible. This "αG" coupling is much larger than the *GG* effect, and it also exhibits unique dependences on input beam polarisation and material handedness – namely, $\Delta E^{(\alpha G)}_{\mathrm{Lin}} = 0$ and $\Delta E^{\alpha G}_{\mathrm{Circ(L)}} = -\Delta E^{\alpha G}_{\mathrm{Circ(R)}}$. If both A and B are of opposite handedness (one R and one L), the discriminatory αG binding energy is zero. The possible configurations of the chiral pair, along with the circularly polarised input light, are provided in Figure 10.

A potential application of these optomechanical forces is for chiral sorting. Although a host of established methods exists for chiral resolution at the molecular level, these methods generally rely on other chiral molecules or other materials to act as resolving agents. Studies utilising optical methods have identified optical trapping forces as a potential tool in the separation of left- and right-handed molecules [107–109], and optical binding forces can contribute to these forces, as we have seen in unique and important ways.

Another possible application is in the development of detecting and identifying chirality [110] in optically bound systems. For example, consider an input laser beam that is modulated between right- and left-handed circular polarisations: the response of a system comprising chiral particles with the same handedness will be an oscillation from their equilibrium positions. If the modulation frequency of the laser is tuned to resonance with the essentially harmonic natural frequency of the optically bound pair [111], the small-scale oscillations should become readily detectable. Treating the αG chiral optical binding effect as a correction to the standard α^2 coupling produces graphs of the form given in Figure 11. In producing the graph, the magnitude of the discriminatory term αG is taken to be of the order of the fine structure constant. It emerges that for a laser wavelength of 628 nm, there is a displacement of 5 nm between these minima. This verifies that a modulation of optical input between circular polarisations will produce a corresponding oscillation in their equilibrium positions [112].

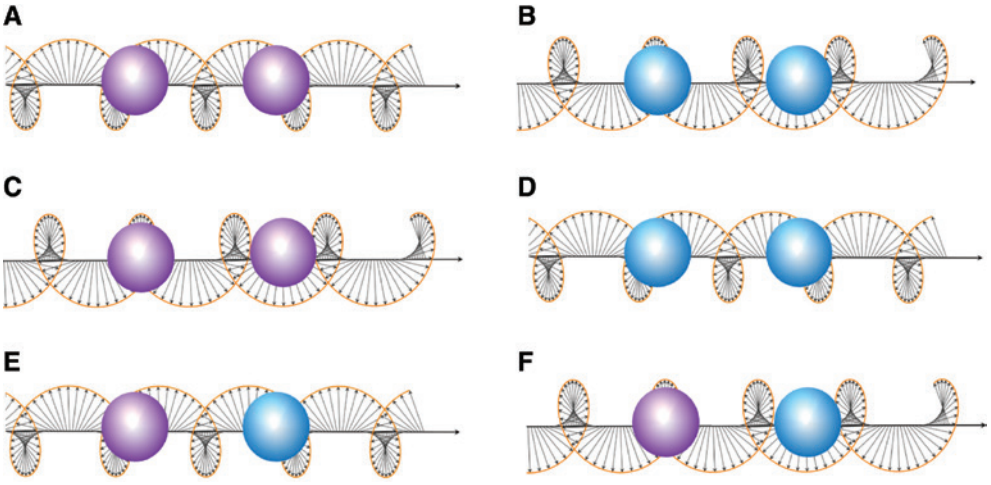

Figure 10: Interplay in differing combinations of optical and material handedness in optically bound pairs of chiral nanoparticles. Illustration of the equivalences (A) ≡ (B) and (C) ≡ (D), and non-equivalences (A), (B) ≠ (C), (D), between the discriminatory optical binding forces for chiral particles of different handedness (depicted by purple and blue spheres) irradiated by circularly polarised light of either handedness (right- and left-handed forms shown with opposite twist). For cases (E), (F), where the two molecules are an enantiomeric pair, the αG discriminatory force vanishes.

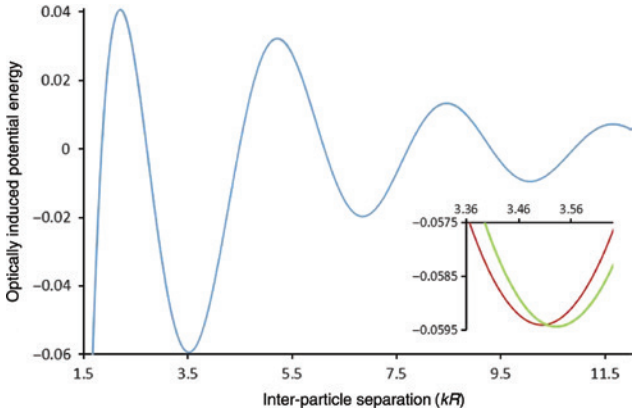

Figure 11: Plot of optical binding potential energy (arbitrary units) for two chiral particles subjected to circularly polarised laser light. The inter-particle separation R is measured in dimensionless units of kR (where $k = 2\pi/\lambda$ with λ the wavelength of incident light). Inset shows the difference between the results for a pair of particles handedness of which is the same or opposite to that of the radiation, around the position of the first potential energy minimum in the main graph. Reproduced with permission from [112].

2.7 Collapse of optical binding

As has been established, optical binding will – under suitable conditions – produce interaction forces that are sufficient to dictate the equilibrium configuration of systems of micron and sub-micron particles. Once an equilibrium is established, such systems are normally quite stable unless there is some perturbation in the input fields (or in the local flow dynamics of the host medium). But even in stable conditions, it proves possible to exert control, and even completely disrupt an optically bound system, by the input of an additional beam that exerts a cancelling effect. To understand how this works, we need to look again at the structure of the electrodynamic coupling tensor.

The coupling that mediates all pairwise optical binding interactions displays a key difference in symmetry properties when its near-field and far-field forms are compared – these distinctions prove to have interesting consequences. It is immediately evident that the tensor expression given by Eq. (2) is cast in an essentially axial form, as is determined by its dependence on the single physical displacement vector $\boldsymbol{R}$. In fact, as the detailed theory shows, the R^{-1} term, which dominates the coupling tensor over all distances beyond the sub-wavelength near-zone, also contains a non-zero isotropic contribution to its essentially axial form – but the R^{-3} and R^{-2} terms have precisely zero isotropic parts [113, 114].

It is possible to obtain a sense of the physics here on the grounds of relative dimensions, taking into account the electrodynamic properties of the nanoparticles between which couplings arise. At short distances, the region between any adjacent nanoparticle pair will be strongly influenced by the secondary fields these nanoparticles produce, through their polarisability interactions with throughput light. However, at more remote distances, inter-particle regions will be less distorted from the electrodynamic isotropy of free space.

Suppose, then, that such a system is subjected to a throughput of optical radiation that is itself of isotropic form (we shall see that there is more than one way to achieve such a condition). Then, since the isotropic part of the coupling potential is supported only in the far-field, it is only in this region that optical binding effects can be produced. This is, indeed, what the theory shows: under these conditions, the major terms supporting optical binding entirely vanish in the short, sub-wavelength region, leaving only an R^{-1} attraction that is much less significant (by a factor of k^2R^2). Essentially, only the long-range interaction is sustained under isotropic conditions. This is a principle that has already found application in a very different sphere of application, namely Bose-Einstein condensates [115].

To achieve the necessary conditions of local field isotropy, there are various scenarios. The simplest is to set up two optical beams of the same wavelength, at right angles to each other, intersecting at the target volume. One beam should be unpolarised, and the other, of twice the intensity, linearly polarised in the plane defined by the two beams. Another alternative is to replace the unpolarised beam with two counter-propagating beams of orthogonal linear polarisation. By increasing the intensity of the side-beam, from below the condition of equal intensities, there is a threshold at which a stable, optically bound assembly of particles will fall apart. Therefore, there is a possibility of deforming and collapsing optically bound multi-particle assemblies by introducing additional sources of laser light [116]. By controlling the irradiances of primary and secondary counter-propagating laser beams, nanoparticles can be assembled into lamellar-type arrays, extended linear chains can subsequently be made to collapse and contract, and nanoparticles can even be made to agglomerate. This possibility has also been entertained theoretically for optical binding between ultra-cold atoms [117].

2.8 Plasmonic near-field optical binding

A relatively new research avenue has been developed in relation to laser-induced optical forces, which is known

as *near-field plasmonic optical binding*. Here, plasmonic nanoparticles are separated by nanometre distances $R \ll \lambda$, rather than the micrometres of the intermediate field $R \approx \lambda$ characteristic of standard optical binding; plasmonic particles in the latter region do not interact. In such circumstances, the surface plasmons in metallic nanoparticles can couple directly to one another, and large binding forces between two plasmonic nanoparticles can arise [118]. Employing an electrodynamical approach that includes retardation effects, with input light intensities at around 10^{10} W m^{-2}, optical forces are found in the nano-Newton range [119]. Reinforcing this research, calculations using the Mie theory and the Lorentz force (combined with the Maxwell stress tensor formalism) determine similar results [120, 121]. Further studies have examined the optical forces between a plasmonic disk and a plasmonic ring [122], head-to-tail aligned gold nanorods [123] and plasmonic nanocubes [124]. In these later works, it was discovered that the optical binding force can be *reversed* (from attractive to repulsive and *vice versa*) when approaching a dipole-multipole Fano resonance, which cannot be described by the Lorentz formula [125], and it vanishes at inter-particle separations beyond 100 nm [126]. Complete control of this reversal in the near-field binding force is now the target, which would be useful for potential manufacture of the "optical matter" of plasmonic nanoparticles.

2.9 Further applications of optical binding

Strong optical binding forces have been observed to play a key role in the intrinsic self-healing property of so-called "metamolecules" (collections of silver nanoparticles that come in different isomers) which, after a perturbation that breaks or deforms the structure, is seen to reconstruct itself (Figure 12) [127].

Another technique which utilises nanoscale optical binding involves hybrid nanoparticle assemblies. In these systems an optically bound chain of metallic nanoparticles produces strong and locally enhanced electromagnetic fields near the chain, which can then co-trap small and less polarisable particles such as quantum dots and smaller metallic particles on intermediate and near-field scales [128]. Finally, it has been shown how, by controlling optically bound arrays of nanoparticles by their cluster size, configuration and separations, the optical torque they experience from an incident beam with optical angular momentum can again be controlled and switched between positive to negative [129].

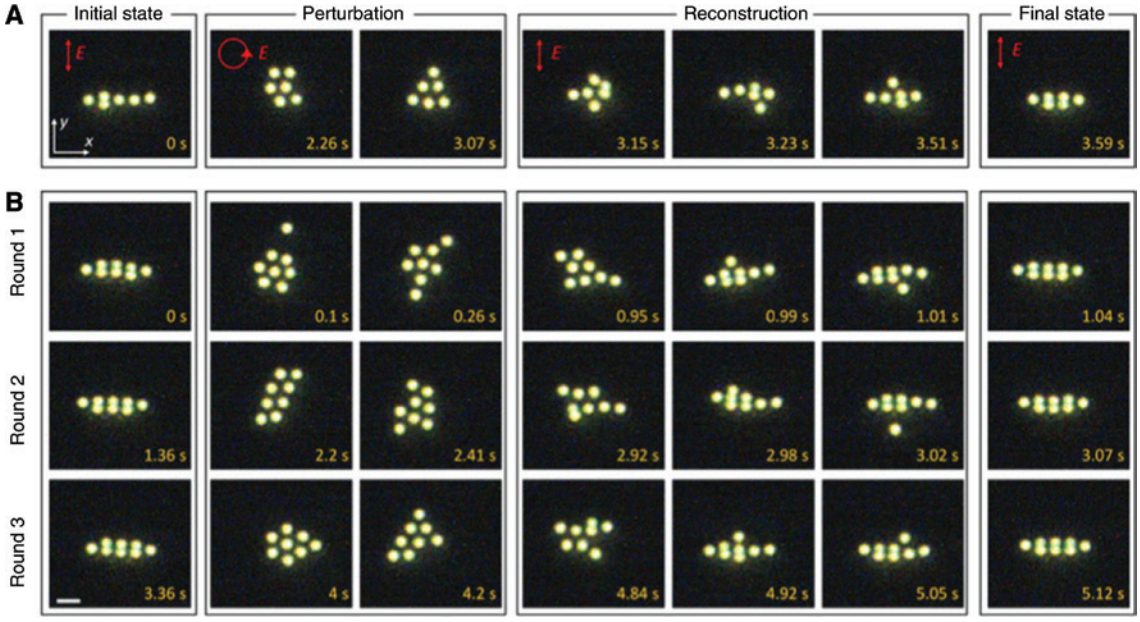

Figure 12: Dark-field optical images of light-driven self-healing of quasi-one-dimensional silver nanoparticle-based metamolecules. (A) and (B) show several silver 150 nm nanoparticles self-assembled into metamolecules using a linearly polarised optical field (first column), then transformed into unstable structures upon external perturbations (by changing from linear to circularly polarised light, second and third columns), and finally reconstructed into (A) a shorter metamolecule with two dimer units and (B) the same configurations as the initial state when the polarisation is changed back to the linearly polarised state (columns 4–7). The scale bar is 1 μm. Reproduced with permission from [127].

3 Conclusion

In this Review, we have concisely surveyed a collection of the most recent developments in optical binding at the nanoscale. It is worth re-emphasising that, in each case, there is no change in the photonic mode population for the specifically off-resonant laser beam, despite its capacity to exert control over local material interactions. It is in this sense that the off-resonant nanophotonic effect of optical binding can be thought of as a form of optical catalysis – an effect in which the additional element expedites a process without itself suffering loss or change. There are also several different forms of off-resonance nanophotonic effects, each of which specifically involves real electronic transitions. The interest here primarily focuses on new elements of control of resonance energy transfer [130], fluorescence [131] and absorption [132], several of which may offer novel routes to all-optical switching [133, 134] and an optical transistor [135]. As such, the key aspect of these processes is a rate – the speed at which change can be registered – as opposed to most equilibrium-oriented applications of optical binding [136]. As was originally the case with optical binding at the nanoscale, theoretical work is racing ahead of experimental observations at present. Fuller details of all these activation processes are given in our very recent review [137].

Experimental studies on nanoscale optical binding are right now starting to bear fruit in a variety of applications. Potential energy landscape surfaces have been generated to determine the position of nanoparticles in the optical field, while simulations can accurately forecast the observed pattern of multi-nanoparticle assemblies of optical matter. It is now known that additional optical binding features arise when complex forms of light are introduced, the potential being heightened when the nanoparticles are non-spherical, and even more so when they are chiral. Such effects are also proving to offer optically tailored routes to the self-assembly of structured nanoscale materials. Scaling up these effects, especially in films and on surfaces, may provide new elements of control in metamaterials, and perhaps even 3D printing. For example, on a suitable substrate, it is already possible by existing means to produce highly polarisation-selective optical characteristics – including, in the case of chiral structures, a remarkable differentiation between circular polarisations [138, 139].

At present, much of the most effective work on optical binding at the nanoscale relies on the enhanced coupling of light-matter interactions afforded by localised surface plasmons, another distinct area of research that is currently proliferating at a remarkable rate [140–142]. When nanofabrication accommodates the effects of optically induced local forces, new directions may be expected to emerge. Device applications are already being pursued following the report of groundbreaking production of a completely flat, high numerical aperture, high definition lens from an ordered array of nanoscale TiO_2 nanoparticles [143]. In another recent application of optical binding, it has also been shown how optically induced forces can play a critical role in determining precise and consistent inter-particle separations of deposited silver nanoparticle chains and arrays onto solid substrates in so-called "optical printing" [144] – a potentially important fabrication technique for creating new photonic devices.

In conclusion, we have seen that the ability to observe optical binding in nanoparticles has now been experimentally secured in a wide variety of implementations. Moreover, a promising range of applications is now starting to be identified. The future for optical binding in nanophotonics appears a truly bright prospect.

Acknowledgements: K.A.F would like to thank the Leverhulme Trust for funding him through a Leverhulme Early Career Fellowship.

Funding: Leverhulme Trust, Grant Number: ECF-2019-398.

References

[1] Kirchhoff G. Ueber die Fraunhofer'schen Linien. Ann Phys (Berlin) 1860;185:148–50.
[2] Kirchhoff G. Ueber das Verhältniss zwischen dem Emissionsvermögen und dem Absorptionsvermögen der Körper für Wärme und Licht. Ann Phys (Berlin) 1860;185:275–301.
[3] Einstein A. Strahlungs-Emission und -Absorption nach der Quantentheorie. Verh Deutsch Phys Gesell 1916;18:318–23.
[4] Einstein A. Zur Quantentheorie der Strahlung. Phys Zeit 1917;18:121–8.
[5] Kaiser W, Garrett CGB. Two-photon excitation in CaF_2:Eu^{2+}. Phys Rev Lett 1961;7:229–31.
[6] Abella ID. Optical double-photon absorption in cesium vapor. Phys Rev Lett 1962;9:453–5.
[7] Braunstein R, Ockman N. Optical double-photon absorption in CdS. Phys Rev 1964;134:A499–507.
[8] Göppert-Mayer M. Über Elementarakte mit zwei Quantensprüngen. Ann Phys (Berlin) 1931;401:273–94.
[9] Franken PA, Hill AE, Peters CW, Weinreich G. Generation of optical harmonics. Phys Rev Lett 1961;7:118–9.
[10] Maker PD, Terhune RW, Savage CM. Intensity-dependent changes in the refractive index of liquids. Phys Rev Lett 1964;12:507–9.
[11] Ashkin A. Acceleration and trapping of particles by radiation pressure. Phys Rev Lett 1970;24:156–9.

[12] Dalibard J, Cohen-Tannoudji C. Laser cooling below the Doppler limit by polarization gradients: simple theoretical models. J Opt Soc Am B 1989;6:2023–45.
[13] Babiker M, Power WL, Allen L. Light-induced torque on moving atoms. Phys Rev Lett 1994;73:1239–42.
[14] Grier DG. A revolution in optical manipulation. Nature 2003;424:810–6.
[15] Maragò OM, Jones PH, Gucciardi PG, Volpe G, Ferrari AC. Optical trapping and manipulation of nanostructures. Nat Nanotechnol 2013;8:807–19.
[16] Bradshaw DS, Andrews DL. Manipulating particles with light: radiation and gradient forces. Eur J Phys 2017;38:034008.
[17] Bradac C. Nanoscale optical trapping: a review. Adv Opt Mater 2018;6:1800005.
[18] Favre-Bulle IA, Stilgoe AB, Scott EK, Rubinsztein-Dunlop H. Optical trapping in vivo: theory, practice, and applications. Nanophoton 2019;8:1023–40.
[19] Babiker M, Andrews DL, Lembessis VE. Atoms in complex twisted light. J Opt 2019;21:013001.
[20] Andrews DL, Bradshaw DS. Optical nanomanipulation. San Rafael, CA, Morgan & Claypool Publishers, 2016.
[21] Dholakia K, Zemanek P. Gripped by light: optical binding. Rev Mod Phys 2010;82:1767–91.
[22] Bradshaw DS, Andrews DL. Optically induced forces and torques: Interactions between nanoparticles in a laser beam. Phys Rev A 2005;72:033816.
[23] Thirunamachandran T. Intermolecular interactions in the presence of an intense radiation field. Mol Phys 1980;40:393–9.
[24] Milonni PW, Shih ML. Source theory of the Casimir force. Phys Rev A 1992;45:4241–53.
[25] Dapasse F, Vigoureux JM. Optical binding force between two Rayleigh particles. J Phys D: Appl Phys 1994;27:914–9.
[26] Milonni PW, Smith A. van der Waals dispersion forces in electromagnetic fields. Phys Rev A 1996;53:3484–9.
[27] Chaumet PC, Nieto-Vesperinas M. Optical binding of particles with or without the presence of a flat dielectric surface. Phys Rev B 2001;64:035422.
[28] Nieto-Vesperinas M, Chaumet PC, Rahmani A. Near-field photonic forces. Philos Trans R Soc A 2004;362:719–37.
[29] Burns MM, Fournier J-M, Golovchenko JA. Optical binding. Phys Rev Lett 1989;63:1233–6.
[30] Burns MM, Fournier J-M, Golovchenko JA. Optical matter: crystallization and binding in intense optical fields. Science 1990;249:749–54.
[31] Mohanty SK, Andrews JT, Gupta PK. Optical binding between dielectric particles. Opt Express 2004;12:2746–53.
[32] Bowman RW, Padgett MJ. Optical trapping and binding. Rep Prog Phys 2013;76:026401.
[33] Jones PH, Maragò OM, Volpe G. Optical tweezers: principles and applications. Cambridge, Cambridge University Press, 2015.
[34] Čižmár T, Dávila Romero LC, Dholakia K, Andrews DL. Multiple optical trapping and binding: new routes to self-assembly. J Phys B: Atom Mol Opt Phys 2010;43:102001.
[35] Andrews DL, Bradshaw DS. The role of virtual photons in nanoscale photonics. Ann Phys (Berlin) 2014;526:173–86.
[36] Lvovsky AI, Mlynek J. Quantum-optical catalysis: generating nonclassical states of light by means of linear optics. Phys Rev Lett 2002;88:250401.
[37] Hu L-Y, Wu J-N, Liao Z, Zubairy MS. Multiphoton catalysis with coherent state input: nonclassicality and decoherence. J Phys B: Atom Mol Opt Phys 2016;49:175504.
[38] Hu L, Liao Z, Zubairy MS. Continuous-variable entanglement via multiphoton catalysis. Phys Rev A 2017;95:012310.
[39] Zhou W, Ye W, Liu C, Hu L, Liu S. Entanglement improvement of entangled coherent state via multiphoton catalysis. Laser Phys Lett 2018;15:065203.
[40] Hilsabeck KI, Meiser JL, Sneha M, Harrison JA, Zare RN. Non-resonant photons catalyze photodissociation of phenol. J Am Chem Soc 2019;141:1067–73.
[41] Salam A. Intermolecular interactions in a radiation field via the method of induced moments. Phys Rev A 2006;73:013406.
[42] Daniels GJ, Jenkins RD, Bradshaw DS, Andrews DL. Resonance energy transfer: the unified theory revisited. J Chem Phys 2003;119:2264–74.
[43] Sukhov S, Shalin A, Haefner D, Dogariu A. Actio et reactio in optical binding. Opt Express 2015;23:247–52.
[44] Chvátal L, Brzobohatý O, Zemánek P. Binding of a pair of Au nanoparticles in a wide Gaussian standing wave. Opt Rev 2015;22:157–61.
[45] Liaw J-W, Kuo T-Y, Kuo M-K. Plasmon-mediated binding forces on gold or silver homodimer and heterodimer. J Quant Spectrosc Radiat Transfer 2016;170:150–8.
[46] Salam A. Two alternative derivations of the static contribution to the radiation-induced intermolecular energy shift. Phys Rev A 2007;76:063402.
[47] Juzeliūnas G. Molecule-radiation and molecule-molecule processes in condensed media: a microscopic QED theory. Chem Phys 1995;198:145–58.
[48] Juzeliūnas G. Microscopic theory of quantization of radiation in molecular dielectrics: normal-mode representation of operators for local and averaged (macroscopic) fields. Phys Rev A 1996;53:3543–58.
[49] Juzeliūnas G. Microscopic theory of quantization of radiation in molecular dielectrics. II. Analysis of microscopic field operators. Phys Rev A 1997;55:929–34.
[50] Rodríguez J, Dávila Romero LC, Andrews DL. Optical binding in nanoparticle assembly: potential energy landscapes. Phys Rev A 2008;78:043805.
[51] Demergis V, Florin E-L. Ultrastrong optical binding of metallic nanoparticles. Nano Lett 2012;12:5756–60.
[52] Yan Z, Shah RA, Chado G, Gray SK, Pelton M, Scherer NF. Guiding spatial arrangements of silver nanoparticles by optical binding interactions in shaped light fields. ACS Nano 2013;7:1790–802.
[53] Koenderink AF, Alù A, Polman A. Nanophotonics: shrinking light-based technology. Science 2015;348:516–21.
[54] Yan Z, Bao Y, Manna U, Shah RA, Scherer NF. Enhancing nanoparticle electrodynamics with gold nanoplate mirrors. Nano Lett 2014;14:2436–42.
[55] Nan F, Yan Z. Probing spatiotemporal stability of optical matter by polarization modulation. Nano Lett 2018;18:1396–401.
[56] Demergis V, Florin E-L. High precision and continuous optical transport using a standing wave optical line trap. Opt Express 2011;19:20833–48.
[57] Bradshaw DS, Forbes KA, Andrews DL. Sculpting optical energy landscapes for multi-particle nanoscale assembly. Proc SPIE 2014;9126:91260P.
[58] Nan F, Yan Z. Silver-nanowire-based interferometric optical tweezers for enhanced optical trapping and binding of nanoparticles. Adv Funct Mater 2019;29:1808258.
[59] Nan F, Yan Z. Tuning nanoparticle electrodynamics by an optical-matter-based laser beam shaper. Nano Lett 2019;19:3353–8.

[60] Jaquay E, Martínez LJ, Mejia CA, Povinelli ML. Light-assisted, templated self-assembly using a photonic-crystal slab. Nano Lett 2013;13:2290–4.
[61] Mejia CA, Dutt A, Povinelli ML. Light-assisted templated self assembly using photonic crystal slabs. Opt Express 2011;19:11422–8.
[62] Huang N, Martínez LJ, Jaquay E, Nakano A, Povinelli ML. Optical epitaxial growth of gold nanoparticle arrays. Nano Lett 2015;15:5841–5.
[63] Dávila Romero LC, Rodríguez J, Andrews DL. Electrodynamic mechanism and array stability in optical binding. Opt Commun 2008;281:865–70.
[64] Yan Z, Gray SK, Scherer NF. Potential energy surfaces and reaction pathways for light-mediated self-organization of metal nanoparticle clusters. Nat Commun 2014;5:3751.
[65] Dávila Romero LC, Andrews DL. Geometric configurations and perturbative mechanisms in optical binding. Proc SPIE 2010;7613:76130P.
[66] Karásek V, Čižmár T, Brzobohatý O, Zemánek P, Garcés-Chávez V, Dholakia K. Long-range one-dimensional longitudinal optical binding. Phys Rev Lett 2008;101:143601.
[67] Kostina N, Petrov M, Ivinskaya A, et al. Optical binding via surface plasmon polariton interference. Phys Rev B 2019;99:125416.
[68] Nan F, Han F, Scherer NF, Yan Z. Dissipative self-assembly of anisotropic nanoparticle chains with combined electrodynamic and electrostatic interactions. Adv Mater 2018;30:1803238.
[69] Kudo T, Yang S-J, Masuhara H. A single large assembly with dynamically fluctuating swarms of gold nanoparticles formed by trapping laser. Nano Lett 2018;18:5846–53.
[70] Taflove A, Hagness SC. Computational electrodynamics: the finite-difference time-domain method, 3rd ed. Norwood, MA, Artech House, 2005.
[71] Sule N, Rice SA, Gray SK, Scherer NF. An electrodynamics-Langevin dynamics (ED-LD) approach to simulate metal nanoparticle interactions and motion. Opt Express 2015;23:29978–92.
[72] McCormack P, Han F, Yan Z. Self-organization of metal nanoparticles in light: electrodynamics–molecular dynamics simulations and optical binding experiments. J Phys Chem Lett 2018;9:545–9.
[73] Grzegorczyk TM, Rohner J, Fournier J-M. Optical mirror from laser-trapped mesoscopic particles. Phys Rev Lett 2014;112:023902.
[74] Yao AM, Padgett MJ. Orbital angular momentum: origins, behavior and applications. Adv Opt Photon 2011;3:161–204.
[75] Andrews DL, Babiker M. The angular momentum of light. Cambridge, UK, Cambridge University Press, 2013.
[76] Barnett SM, Babiker M, Padgett MJ. Optical orbital angular momentum. Philos Trans R Soc A 2017;375:20150444.
[77] He H, Friese MEJ, Heckenberg NR, Rubinsztein-Dunlop H. Direct observation of transfer of angular-momentum to absorptive particles from a laser-beam with a phase singularity. Phys Rev Lett 1995;75:826–9.
[78] Friese MEJ, Enger J, Rubinsztein-Dunlop H, Heckenberg NR. Optical angular-momentum transfer to trapped absorbing particles. Phys Rev A 1996;54:1593–6.
[79] Simpson NB, Allen L, Padgett MJ. Optical tweezers and optical spanners with Laguerre-Gaussian modes. J Mod Opt 1996;43:2485–91.
[80] Simpson NB, Dholakia K, Allen L, Padgett MJ. Mechanical equivalence of spin and orbital angular momentum of light: an optical spanner. Opt Lett 1997;22:52–4.
[81] Roichman Y, Grier DG, Zaslavsky G. Anomalous collective dynamics in optically driven colloidal rings. Phys Rev E 2007;75:020401.
[82] Molloy JE, Padgett MJ. Lights, action: optical tweezers. Contemp Phys 2002;43:241–58.
[83] Padgett M, Bowman R. Tweezers with a twist. Nat Photonics 2011;5:343–8.
[84] Bradshaw DS, Andrews DL. Interactions between spherical nanoparticles optically trapped in Laguerre-Gaussian modes. Opt Lett 2005;30:3039–41.
[85] Dienerowitz M, Mazilu M, Reece PJ, Krauss TF, Dholakia K. Optical vortex trap for resonant confinement of metal nanoparticles. Opt Express 2008;16:4991–9.
[86] Donato MG, Brzobohatý O, Simpson SH, et al. Optical trapping, optical binding, and rotational dynamics of silicon nanowires in counter-propagating beams. Nano Lett 2019;19:342–52.
[87] Figliozzi P, Sule N, Yan Z, et al. Driven optical matter: dynamics of electrodynamically coupled nanoparticles in an optical ring vortex. Phys Rev E 2017;95:022604.
[88] Figliozzi P, Peterson CW, Rice SA, Scherer NF. Direct visualization of barrier crossing dynamics in a driven optical matter system. ACS Nano 2018;12:5168–75.
[89] Yan Z, Sajjan M, Scherer NF. Fabrication of a material assembly of silver nanoparticles using the phase gradients of optical tweezers. Phys Rev Lett 2015;114:143901.
[90] Coursault D, Sule N, Parker J, Bao Y, Scherer NF. Dynamics of the optically directed assembly and disassembly of gold nanoplatelet arrays. Nano Lett 2018;18:3391–9.
[91] Peterson CW, Parker J, Rice SA, Scherer NF. Controlling the dynamics and optical binding of nanoparticle homodimers with transverse phase gradients. Nano Lett 2019;19:897–903.
[92] Smith SN, Coles MM, Andrews DL. Optical binding with anisotropic particles: resolving the forces and torques. Proc SPIE 2011;8097:80971E.
[93] Endo M, Iijima S, Dresselhaus MS. Carbon nanotubes. Oxford, Elsevier, 2013.
[94] De Volder MFL, Tawfick SH, Baughman RH, Hart AJ. Carbon nanotubes: present and future commercial applications. Science 2013;339:535–9.
[95] Andrews DL, Bradshaw DS. Laser-induced forces between carbon nanotubes. Opt Lett 2005;30:783–5.
[96] Sun C-H, Yin L-C, Li F, Lu G-Q, Cheng H-M. Van der Waals interactions between two parallel infinitely long single-walled nanotubes. Chem Phys Lett 2005;403:343–6.
[97] Simpson SH, Zemánek P, Maragò OM, Jones PH, Hanna S. Optical binding of nanowires. Nano Lett 2017;17:3485–92.
[98] Andrews DL, Crisp RG, Bradshaw DS. Optically induced inter-particle forces: from the bonding of dimers to optical electrostriction in molecular solids. J Phys B: Atom Mol Opt Phys 2006;39:S637–S50.
[99] Lu H, Liu X, Wang L, Gong Y, Mao D. Ultrafast all-optical switching in nanoplasmonic waveguide with Kerr nonlinear resonator. Opt Express 2011;19:2910–5.
[100] Somasundram K, Amos RD, Handy NC. Ab initio calculation for properties of hydrogen bonded complexes H3N···HCN, HCN···HCN, HCN···HF, H2O···HF. Theor Chem Acc 1986;69:491–503.

[101] Salam A. On the effect of a radiation field in modifying the intermolecular interaction between two chiral molecules. J Chem Phys 2006;124:014302.
[102] Craig D, Thirunamachandran T. New approaches to chiral discrimination in coupling between molecules. Theor Chem Acc 1999;102:112–20.
[103] Salam A. Molecular quantum electrodynamics: long-range intermolecular interactions. Hoboken, NJ, Wiley, 2010.
[104] Cameron RP, Barnett SM, Yao AM. Discriminatory optical force for chiral molecules. New J Phys 2014;16:013020.
[105] Bradshaw DS, Andrews DL. Chiral discrimination in optical trapping and manipulation. New J Phys 2014;16:103021.
[106] Forbes KA, Andrews DL. Chiral discrimination in optical binding. Phys Rev A 2015;91:053824.
[107] Bradshaw DS, Andrews DL. Laser optical separation of chiral molecules. Opt Lett 2015;40:677–80.
[108] Zhao Y, Saleh AAE, Dionne JA. Enantioselective optical trapping of chiral nanoparticles with plasmonic tweezers. ACS Photonics 2016;3:304–9.
[109] Zhao Y, Saleh AAE, van de Haar MA, et al. Nanoscopic control and quantification of enantioselective optical forces. Nat. Nanotechnol 2017;12:1055.
[110] Zhao Y, Askarpour AN, Sun L, Shi J, Li X, Alù A. Chirality detection of enantiomers using twisted optical metamaterials. Nat Commun 2017;8:14180.
[111] Metzger NK, Marchington RF, Mazilu M, Smith RL, Dholakia K, Wright EM. Measurement of the restoring forces acting on two optically bound particles from normal mode correlations. Phys Rev Lett 2007;98:068102.
[112] Bradshaw DS, Forbes KA, Leeder JM, Andrews DL. Chirality in optical trapping and optical binding. Photonics 2015;2:483–97.
[113] Scholes GD, Andrews DL. Damping and higher multipole effects in the quantum electrodynamical model for electronic energy transfer in the condensed phase. J Chem Phys 1997;107:5374–84.
[114] Andrews DL. On the conveyance of angular momentum in electronic energy transfer. Phys Chem Chem Phys 2010;12:7409–17.
[115] O'Dell D, Giovanazzi S, Kurizki G, Akulin V. Bose-Einstein condensates with 1/r interatomic attraction: Electromagnetically induced "gravity". Phys Rev Lett 2000;84:5687.
[116] Andrews DL, Rodríguez J. Collapse of optical binding under secondary irradiation. Opt Lett 2008;33:1830–2.
[117] Máximo CE, Bachelard R, Kaiser R. Optical binding with cold atoms. Phys Rev A 2018;97:043845.
[118] Zelenina AS, Quidant R, Nieto-Vesperinas M. Enhanced optical forces between coupled resonant metal nanoparticles. Opt Lett 2007;32:1156–8.
[119] Ng J, Tang R, Chan CT. Electrodynamics study of plasmonic bonding and antibonding forces in a bisphere. Phys Rev B 2008;77:195407.
[120] Miljković VD, Pakizeh T, Sepulveda B, Johansson P, Käll M. Optical forces in plasmonic nanoparticle dimers. J Phys Chem C 2010;114:7472–9.
[121] Salary MM, Mosallaei H. Tailoring optical forces for nanoparticle manipulation on layered substrates. Phys Rev B 2016;94:035410.
[122] Zhang Q, Xiao JJ. Multiple reversals of optical binding force in plasmonic disk-ring nanostructures with dipole-multipole Fano resonances. Opt Lett 2013;38:4240–3.
[123] Zhang Q, Xiao JJ, Zhang XM, Yao Y, Liu H. Reversal of optical binding force by Fano resonance in plasmonic nanorod heterodimer. Opt Express 2013;21:6601–8.
[124] Mahdy MRC, Zhang T, Danesh M, Ding W. Substrate and Fano resonance effects on the reversal of optical binding force between plasmonic cube dimers. Sci Rep 2017;7:6938.
[125] Gallinet B, Martin OJF. Ab initio theory of Fano resonances in plasmonic nanostructures and metamaterials. Phys Rev B 2011;83:235427.
[126] Rivy HM, Mahdy MRC, Jony ZR, Masud N, Satter SS, Jani R. Plasmonic or dielectric dimers: a generic way to control the reversal of near field optical binding force. Opt Commun 2019;430:51–62.
[127] Nan F, Yan Z. Light-driven self-healing of nanoparticle-based metamolecules. Angew Chem Int Ed 2019;58:4917–22.
[128] Yan Z, Manna U, Qin W, Camire A, Guyot-Sionnest P, Scherer NF. Hierarchical photonic synthesis of hybrid nanoparticle assemblies. J Phys Chem Lett 2013;4:2630–6.
[129] Han F, Parker JA, Yifat Y, et al. Crossover from positive to negative optical torque in mesoscale optical matter. Nat Commun 2018;9:4897.
[130] Allcock P, Jenkins RD, Andrews DL. Laser-assisted resonance-energy transfer. Phys Rev A 2000;61:023812.
[131] Bradshaw DS, Andrews DL. Mechanism for optical enhancement and suppression of fluorescence. J Phys Chem A 2009;113:6537–9.
[132] Bradshaw DS, Andrews DL. Laser-modified one- and two-photon absorption: expanding the scope of optical nonlinearity. Phys Rev A 2013;88:033807.
[133] Bradshaw DS, Andrews DL. Optically controlled resonance energy transfer: mechanism and configuration for all-optical switching. J Chem Phys 2008;128:144506.
[134] Bradshaw DS, Andrews DL. All-optical switching between quantum dot nanoarrays. Superlatt Microstruct 2010;47:308–13.
[135] Andrews DL, Bradshaw DS. Off-resonant activation of optical emission. Opt Commun 2010;283:4365–7.
[136] Bradshaw DS, Andrews DL. Interparticle interactions: energy potentials, energy transfer, and nanoscale mechanical motion in response to optical radiation. J Phys Chem A 2013;117:75–82.
[137] Bradshaw DS, Forbes KA, Andrews DL. Off-resonance control and all-optical switching: expanded dimensions in nonlinear optics. Appl Sci 2019;9:4252.
[138] Lakhtakia A, Messier R. Sculptured thin films: nanoengineered morphology and optics. Bellingham, SPIE Press, 2005, Vol. 117.
[139] Fedotov VA, Mladyonov PL, Prosvirnin SL, Rogacheva AV, Chen Y, Zheludev NI. Asymmetric propagation of electromagnetic waves through a planar chiral structure. Phys Rev Lett 2006;97:167401.
[140] Pelton M, Aizpurua J, Bryant G. Metal-nanoparticle plasmonics. Laser Photonics Rev 2008;2:136–59.
[141] Stockman MI. Nanoplasmonics: past, present, and glimpse into future. Opt Express 2011;19:22029–106.
[142] Klimov V. Nanoplasmonics. Boca Raton, FL, Pan Stanford, 2014.
[143] Khorasaninejad M, Chen WT, Devlin RC, Oh J, Zhu AY, Capasso F. Metalenses at visible wavelengths: Diffraction-limited focusing and subwavelength resolution imaging. Science 2016;352:1190–4.
[144] Bao Y, Yan Z, Scherer NF. Optical printing of electrodynamically coupled metallic nanoparticle arrays. J Phys Chem C 2014;118:19315–21.